PNAS RESEARCH ARTICLE | PLANT BIOLOGY

PIF4 enhances the expression of *SAUR* genes to promote growth in response to nitrate

Matías Ezequiel Pereyra[a,b], Cecilia Costigliolo Rojas[b], Anne F. Jarrell[c], Austin S. Hovland[d], Stephen A. Snipes[c], Punita Nagpal[c], David Alabadí[e], Miguel A. Blázquez[e], Rodrigo A. Gutiérrez[f], Jason W. Reed[c], William M. Gray[d], and Jorge José Casal[a,b,1]

Edited by Mark Estelle, University of California, San Diego, CA; received March 18, 2023; accepted August 9, 2023

Nitrate supply is fundamental to support shoot growth and crop performance, but the associated increase in stem height exacerbates the risks of lodging and yield losses. Despite their significance for agriculture, the mechanisms involved in the promotion of stem growth by nitrate remain poorly understood. Here, we show that the elongation of the hypocotyl of *Arabidopsis thaliana*, used as a model, responds rapidly and persistently to upshifts in nitrate concentration, rather than to the nitrate level itself. The response occurred even in shoots dissected from their roots and required NITRATE TRANSPORTER 1.1 (NRT1.1) in the phosphorylated state (but not NRT1.1 nitrate transport capacity) and NIN-LIKE PROTEIN 7 (NLP7). Nitrate increased PHYTOCHROME INTERACTING FACTOR 4 (PIF4) nuclear abundance by posttranscriptional mechanisms that depended on NRT1.1 and phytochrome B. In response to nitrate, PIF4 enhanced the expression of numerous *SMALL AUXIN-UP RNA (SAUR)* genes in the hypocotyl. The growth response to nitrate required PIF4, positive and negative regulators of its activity, including AUXIN RESPONSE FACTORs, and SAURs. PIF4 integrates cues from the soil (nitrate) and aerial (shade) environments adjusting plant stature to facilitate access to light.

NRT1.1 | NLP7 | ARF7 | shade

Significance

Nitrate increases the yield potential of crops but, by enhancing plant stature, it also exacerbates the risk of lodging. During the Green Revolution, the introduction of dwarfing genes alleviated this problem, but at the expense of nitrogen use efficiency. By using the hypocotyl of *Arabidopsis thaliana* as a model, we elucidate the mechanisms by which nitrate promotes plant stature. Hypocotyl elongation responds to nitrate upshifts rather than to the actual levels of the nutrient. Nitrate sensing increases the nuclear abundance of selected transcription factors, which increase the expression of numerous members of the *SAUR* gene family involved in the promotion of cell expansion. The pathway reveals potential targets to genetically reduce plant stature without the drawbacks of current approaches.

Nitrogen levels required to optimize crop yield potential can lead to taller plants with reduced root anchorage relative to the size of the shoot, weaker basal internodes, and hence higher risks of lodging (1). Nitrate-enhanced lodging causes important yield losses in staple crops, including wheat (2), rice (3), maize (4), sunflower (5), and rapeseed (6). During the "Green Revolution" in the 1960s, the introduction of semidwarf varieties of wheat, involving the introgression of stable versions of the growth repressor DELLA proteins, reduced lodging susceptibility and allowed higher rates of nitrogen supply (7, 8). However, this approach decreased nitrogen use efficiency (9–12), forcing the overuse of nitrogen fertilization with the associated negative environmental and economic consequences (13).

In well-aerated soils, nitrogen predominates in the form of nitrate (NO_3^-). Due to its negative charge, this chemical form is mobile, and its levels can fluctuate dramatically (14). Nitrate provides a signal that affects growth and development, and other sources of nitrogen cannot replace this function (15, 16). The NITRATE TRANSPORTER 1.1 (NRT1.1) transceptor is both a dual affinity transporter of nitrate and a nitrate receptor (17–19). Low concentrations of nitrate lead to phosphorylation of the threonine 101 residue and monomerization of the NRT1.1 protein, whereas high concentrations lead to dephosphorylation and dimerization of NRT1.1 (20, 21). Phosphorylation of T101 increases transport affinity (22), but its impact on the sensory function of NRT1.1 is strongly context dependent (17, 19). Nitrate sensed by NRT1.1 triggers cytoplasmic waves of calcium that activate different CALCIUM SENSOR PROTEIN KINASES (CPKs), which in turn phosphorylate the transcription factor NIN-LIKE PROTEIN 7 (NLP7) to induce the expression of multiple nitrate responsive genes, including those related to nitrate transport and assimilation and nitrate-induced growth (23–25). NLP7 is also a nitrate sensor by virtue of a domain conserved in bacteria and cyanobacteria nitrate sensor proteins (26). Full phosphorylation and nuclear retention of NLP7 require the synergistic action caused by nitrate binding and the CPKs pathway (23, 26, 27).

Nitrate effects on root architecture involve NRT1.1, NLP7, and auxin transport and perception (24, 28–31). The promotion of foliage expansion by nitrate involves the induction of endoreplication and the increase in cell size mediated by the cyclin-dependent kinase inhibitor LOSS OF GIANT CELLS FROM ORGANS (*LGO*) (32), the induction of cytokinin synthesis in the root and the enhanced expression of *CYTOKININ RESPONSE FACTOR 2* (*CRF2*), *CRF3,* and *CRF6* and downstream *PIN-FORMED* (*PIN*) genes in

Author contributions: M.E.P. and J.J.C. designed research; M.E.P. and C.C.R. performed research; A.F.J., A.S.H., S.A.S., P.N., J.W.R., and W.M.G. contributed new reagents/analytic tools; D.A., M.A.B., R.A.G., J.W.R., and W.M.G. provided input to the research; M.E.P. and J.J.C. analyzed data; and M.E.P. and J.J.C. wrote the paper.

The authors declare no competing interest.

This article is a PNAS Direct Submission.

[1]To whom correspondence may be addressed. Email: casal@ifeva.edu.ar.

This article contains supporting information online at https://www.pnas.org/lookup/suppl/doi:10.1073/pnas.2304513120/-/DCSupplemental.

Published September 19, 2023.

the cotyledons (33), and the stimulation of the target-of-rapamycin (TOR) pathway by any of several nitrogen sources (34). Despite the effects of nitrogen on stem growth in numerous species (2, 35, 36) and its agricultural relevance due to the increased risk of lodging (2–6), we do not know the mechanisms by which nitrate affects stem growth.

The PHYTOCHROME INTERACTING FACTOR 4 (PIF4), PIF5 (37–39), PIF7 (40–43), AUXIN RESPONSE FACTOR 6 (ARF6), ARF7, ARF8 (44), BRI1-EMS-SUPPRESSOR 1 (BES1), and BRASSINAZOLE-RESISTANT 1 (BZR1) (45, 46) transcription factors share many target genes, are negatively regulated by DELLA proteins (47–50), and play a fundamental function in hypocotyl-growth promotion by neighbor cues and warm temperatures in *Arabidopsis thaliana.* ELONGATED HYPOCOTYL 5 (HY5) competes with PIF4 for promoter binding to antagonistically control its activity (51). Here, we show that nitrate promotes hypocotyl growth in *A. thaliana* via NRT1.1, NLP7, and PIF4, which enhance the expression of numerous *SMALL AUXIN-UP RNA (SAUR)* genes, defining a mechanism that integrates nutrient and growth pathways.

Results

Upshift in Nitrate Availability Promotes Hypocotyl Elongation. We grew Arabidopsis seedlings on agar containing either 0.5 or 5.0 mM potassium nitrate. One hour after the beginning of the photoperiod of the fourth day, we transferred half of the seedlings of each group to the contrasting concentration and the controls to fresh substrate. The hypocotyl growth rate during the remaining 9 h of the photoperiod increased in response to the 0.5 to 5.0 mM upshift (Fig. 1*A*). This promotion was rapid (detectable after 3 h of treatment) and persistent (Fig. 1*B*), resulting in seedlings with longer hypocotyls than those grown on constant nitrate concentrations (*SI Appendix*, Fig. S1*A*). Nitrate also promoted cotyledon expansion (Fig. 1*B*). Continuous growth at 0.5 compared to 5.0 mM nitrate had no effects (Fig. 1*A* and *SI Appendix*, Fig. S1 *A* and *B*), but the shift from 5.0 to 10.0 mM was effective (*SI Appendix*, Fig. S1*C*), suggesting the occurrence of nitrate-induced desensitization. A dose–response curve for hypocotyl growth showed saturation at 10.0 mM potassium nitrate, whereas potassium chloride was ineffective (Fig. 1*C*). Transferring the seedlings to 0.5 mM nitrate plus either ammonium or glutamine to provide the same amount of nitrogen as 5.0 mM nitrate was not effective (Fig. 1*D* and *SI Appendix*, Fig. S1*D*), indicating that the promotion of hypocotyl growth is specific for nitrate. Genetic modification of the TOR pathway (which is induced by diverse nitrogen sources) did not affect the response to nitrate (*SI Appendix*, Fig. S2). Surgically removing the roots did not eliminate the hypocotyl elongation response to the nitrate upshift (Fig. 1*E*).

Nitrate Upshift Sensing by NRT1.1 Promotes Hypocotyl Elongation. The hypocotyls of the *chl1-9* mutant allele of the NRT1.1 transceptor, impaired in nitrate transport but not in

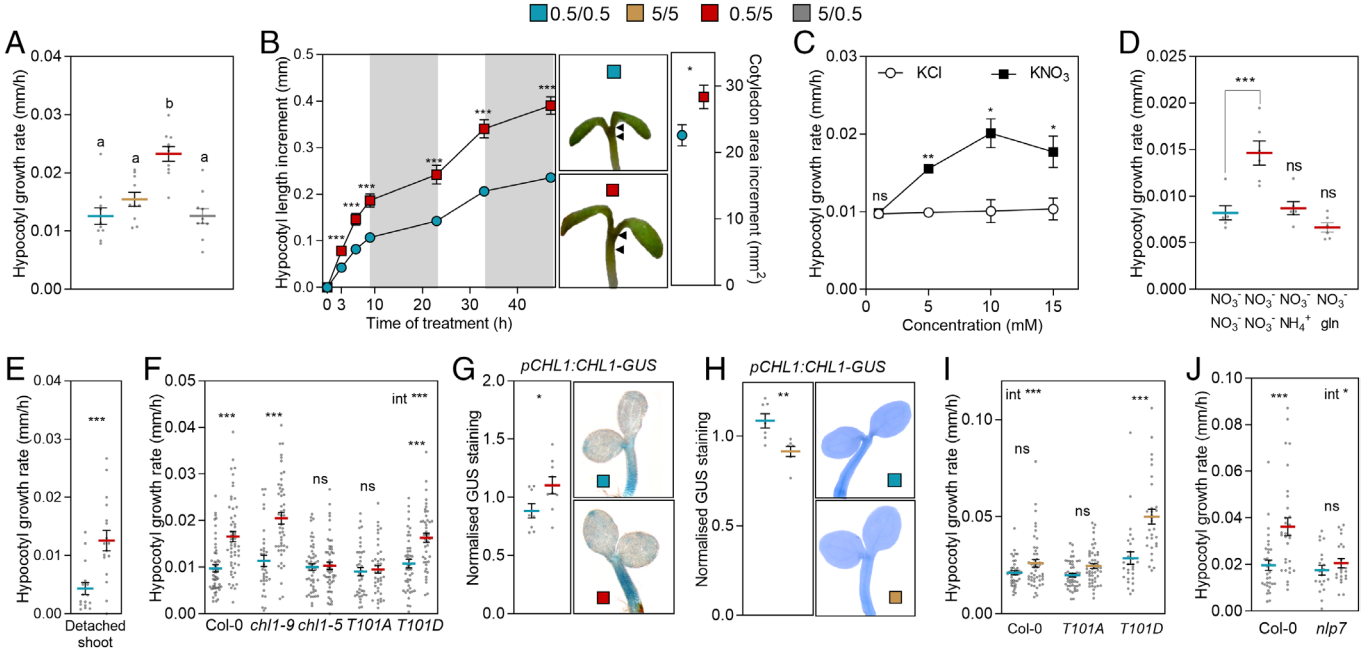

Fig. 1. Nitrate upshifts sensed by NRT1.1 promote hypocotyl growth. (*A*) Hypocotyl growth rate in seedlings grown on 0.5- or 5.0-mM potassium nitrate and either transferred to the contrasting condition or left unchanged, 1 h after the beginning of the photoperiod of day 4 (growth rates measured between 1 and 10 h after the beginning of the photoperiod). (*B*) Kinetics of hypocotyl growth (*Left*) and cotyledon expansion accumulated over the same period (*Right*) after transfer from 0.5 to 5.0 mM nitrate, compared to the control that remained at 0.5 mM nitrate. The arrowheads define length increments in pictures of representative seedling. (*C*) Hypocotyl growth in seedlings transferred from 0.5 mM nitrate to the concentration of potassium nitrate or potassium chloride indicated in abscissas. (*D*) Hypocotyl growth rate in seedlings transferred from 0.5 to 5.0 mM nitrate or to 0.5 mM nitrate plus ammonium or glutamine to provide the equivalent amounts of nitrogen as 5.0 mM nitrate. (*E*) Hypocotyl growth in shoots isolated from their roots 1 h after the beginning of the photoperiod of day 4 and incubated the subsequent 9 h in 0.5- or 5.0-mM nitrate. (*F*) Hypocotyl growth rate in seedlings of the Columbia wild type and the following alleles of *NRT1.1: chl1-9* (deficient in transport), *chl1-5* (null), *chl1-5* complemented with NRT1.1^{T101A} (nonphosphorylatable) and *chl1-5* complemented with NRT1.1^{T101D} (phosphomimetic). (*G*) GUS staining in the hypocotyl driven by the *pCHL1:CHL1-GUS* transgene, 4 h after the shift in nitrate. (*H*) GUS staining in the hypocotyl driven by the *pCHL1:CHL1-GUS* transgene, 5 h after the beginning of the photoperiod of day 4. (*I*) Hypocotyl growth rate in seedlings of the Columbia wild type and the *chl1-5* null mutant complemented with either the NRT1.1^{T101A} (nonphosphorylatable) or NRT1.1^{T101D} (phosphomimetic) alleles. (*J*) Hypocotyl growth in the *nlp7-2* mutant. Data are means ± SE and individual values (*A* and *D–J*) and means ± SE of 7 (*B*) or 3 (*C*) replicate boxes of seedlings. Different letters indicate significant differences ($P < 0.05$) in Tukey tests. Asterisks indicate the significance of the effect of nitrate in Student's *t* tests or Bonferroni tests following significant interaction (int): *$P < 0.05$; **$P < 0.01$; ***$P < 0.001$; ns, not significant.

nitrate sensing (17, 52), showed a wild-type response to the nitrate upshift (Fig. 1*F*). The *chl1-5* allele, impaired both in nitrate transport and sensing, failed to respond (Fig. 1*F*), indicating that the sensing capacity of NRT1.1 mediates the hypocotyl growth response. To investigate the importance of phosphorylation of the regulatory T101 residue, we used the *chl1-5* mutant complemented with either the NRT1.1^{T101A} allele, where a phosphorylatable residue is replaced by a nonphosphorylatable amino acid, or the NRT1.1^{T101D}, which is a phosphomimetic allele. The NRT1.1^{T101A} mutant failed to respond to the nitrate upshift, whereas the NRT1.1^{T101D} showed a wild-type response (Fig. 1*F*), indicating that the promotion of hypocotyl growth requires NRT1.1 phosphorylation at T101. Nitrate treatment rapidly increases the expression of *NRT1.1* in different systems (53–55), and the nitrate upshift enhanced the abundance of NRT1.1 in the hypocotyl, visualized by the protein fused to GUS under the control of the endogenous promoter (Fig. 1*G*). On the contrary, prolonged growth on 5.0 mM nitrate reduced the level of NRT1.1 (Fig. 1*H* and ref. 56), which could contribute to the observed desensitization toward nitrate. We also reasoned that, since the hypocotyl growth response requires NRT1.1 phosphorylation and high nitrate concentration reduced NRT1.1 phosphorylation (17), this could explain in part why prolonged exposure to 5.0 mM nitrate has negligible effects on growth. Consistent with this possibility, the growth of the NRT1.1^{T101D} phosphomimetic allele was higher on continuous 5.0 than 0.5 mM nitrate (Fig. 1*I*). The hypocotyl growth response to nitrate also required NLP7 (Fig. 1*J* and *SI Appendix*, Fig. S3*A*).

The Hypocotyl Elongation Response Requires PIF4, ARF6/ARF7/ARF8, BES1/BZR1, HY5, and DELLAs. The *pif4, arf6 arf7, arf7 arf8, arf6 arf7 arf8, bes1 bzr1*, and *hy5* mutants affected in transcription factors involved in hypocotyl growth responses to shade or warmth, and the *repressor of ga1-3* (*rga*) *gibberellic acid insensitive* (*gai*) loss-of-function and *rga-Δ17* gain of function mutants affected in DELLAs all failed to respond to nitrate (Fig. 2 *A*–*E*). The *pif1*, *pif3*, *pif5*, and *pif7* mutations did not reduce the response, and the combination of *pif5* and *pif7* caused a weak recovery of the response in the *pif4* background (Fig. 2*A*).

Nitrate Upshift Increases PIF4 Nuclear Abundance in Hypocotyl Cells. Prompted by the results of genetic experiments, we analyzed by confocal microscopy the nuclear levels of PIF4, ARF6, ARF7, BES1, HY5, and RGA proteins fused to fluorescent tags under the control of the endogenous promoters in hypocotyl cells. In response to the nitrate upshift, PIF4 and ARF7 increased, whereas ARF6, BES1, and HY5 remained unaffected (Fig. 2*F*). Consistently with previous observations in roots (57), the nitrate upshift enhanced the nuclear levels of RGA in hypocotyl cells (Fig. 2*F*). As DELLAs decrease growth, this mechanism may be a safeguard regulatory feedback loop against excessive elongation. The nitrate upshift also increased PIF4-GFP expressed under the control of the *35S* promoter, indicating the occurrence of posttranscriptional effects, but no response was detected in the *chl1-5* background (Fig. 2*G*).

Nitrate Upshift Increases PIF4 Nuclear Abundance in Cotyledon Cells. Nuclear PIF4-GFP levels also increased in cotyledon cells (Fig. 2*H*). In luminometer readings, dominated by the cotyledons, the nitrate upshift increased PIF4-LUC during the morning and decreased it during the afternoon (Fig. 2 *I* and *J*). The nitrate upshift did not affect the activity of the *PIF4* promoter during the morning (Fig. 2*K*), supporting a posttranscriptional control of PIF4. Consistently with this observation, NLP7 did not affect *PIF4* expression (*SI Appendix*, Fig. S3*B*). The nitrate upshift decreased the activity of the *PIF4* promoter during the afternoon (Fig. 2*K*), suggesting that the negative effect on PIF4-LUC in the cotyledons at this time of the day is mainly due to a transcriptional effect. The promotion of PIF4-LUC by the nitrate upshift was not detectable in the *chl1-5* background, supporting a role of NRT1.1 (Fig. 2*L*). In entire seedlings harvested during the morning (when hypocotyl and cotyledons respond in the same direction), the nitrate upshift enhanced PIF4-HA and PIF4-GFP abundance in protein blots (Fig. 2 *M* and *N*).

The Hypocotyl Elongation Response Requires PIF4 in Hypocotyl and Cotyledon Cells. The nitrate upshift enhanced PIF4 abundance in the cotyledons, which typically results in elevated auxin signaling (37, 39). Surgical excision of the cotyledons reduced the magnitude of the hypocotyl elongation response to nitrate and addition of the synthetic auxin Picloram (5 μM) bypassed the need of these organs, but PIF4 was still required in the hypocotyls treated with Picloram (Fig. 2*O*). In additional experiments, we repositioned excised cotyledons close to the severed petioles of wild-type seedlings without cotyledons. The cotyledons coming from wild-type seedlings restored a partial response to the nitrate upshift but those coming from *pif4* seedlings were not effective (Fig. 2*P*), indicating that PIF4 is required not only in the hypocotyl, but also in the cotyledons.

The Response of PIF4 Requires Active phyB. Similarly to nitrate, the changes in plant architecture induced by canopy shade at high plant population densities increase the risk of lodging in crops (1, 6). The nitrate upshift increased hypocotyl elongation under simulated shade (58) (Fig. 3*A*). Shade reduces the activity of phytochrome B (phyB) and cryptochrome 1 (cry1) photosensory receptors (58–60) and the nitrate upshift promoted growth in the *phyB* or *cry1* mutants under white light (Fig. 3*B*). The effect of the nitrate upshift on PIF4-GFP nuclear levels in hypocotyl cells (Fig. 3*C*) and on the PIF4-LUC during the morning (Fig. 3*D*) persisted in seedlings exposed to shade, but the drop in PIF4-LUC during the afternoon was not apparent (Fig. 3*D*). Since shade leaves residual phyB activity that, combined with cry1 activity, can be biologically effective (61), we investigated whether the nitrate upshift affects growth and PIF4-LUC abundance in seedlings exposed to a long-wavelength pulse of far-red light followed by darkness to virtually eliminate any phyB activity. In contrast to the seedlings exposed to the white light photoperiod (which activates phyB), in those exposed to far-red light, PIF4 levels failed to respond to the nitrate upshift while hypocotyl growth still responded (Fig. 3 *E* and *F*), likely via NLP7. Nuclear phyB forms photobodies by liquid–liquid phase separation, which recruit PIF4 (62). The size of these nuclear bodies is a proxy for phyB activity; the larger the body, the higher the activity (63). We observed a reduction in the number of large phyB nuclear bodies in response to the nitrate upshift under both white light and shade conditions (Fig. 3*G*).

The Nitrate Upshift Enhances the Expression of Selected *SAUR* Genes. Since the nitrate upshift enhances PIF4 protein abundance and the growth response requires PIF4, we analyzed the transcriptome of hypocotyl samples harvested from wild-type and *pif4*-mutant seedlings exposed to the nitrate upshift. The lack of changes in relevant genes did not support a role of the LGO endoreduplication (32) or CRFs–PINs (33) pathways in the promotion of hypocotyl growth reported here (*SI Appendix*, Fig. S4 *A*–*C*). Consistently with the ARF7-VENUS response, nitrate enhanced *ARF7* expression independently of PIF4 (*SI Appendix*, Fig. S4*D*).

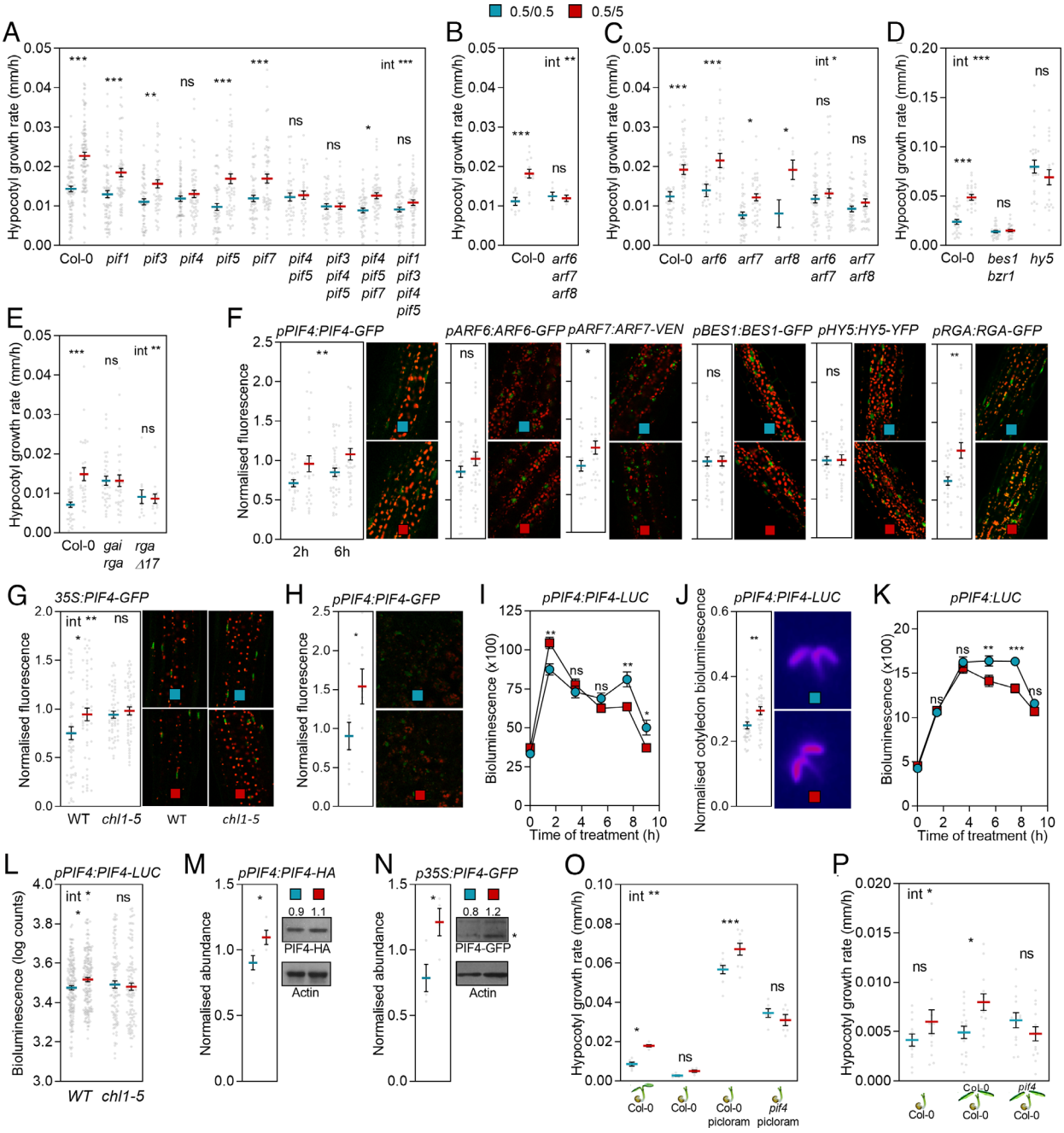

Fig. 2. Nitrate increases PIF4 abundance in hypocotyl and cotyledon cells to promote hypocotyl growth. Seedlings transferred from 0.5 mM to 5.0 mM nitrate 1 h after the beginning of the photoperiod of day 4 are compared to the controls that remained on 0.5 mM nitrate. (*A–E*) Hypocotyl growth rate in seedlings of the wild type, *pif1, pif3, pif4, pif5, pif7* single and multiple mutants (*A*), *arf6, arf7,* and *arf8* single and multiple mutants [*B* and *C*, in *C*, treatments and measurements conducted a day later for all genotypes because these double mutants have elevated growth at earlier stages (44)], *rga gai* and *rga-Δ17* mutants (*E*) 0-9 h after the nitrate upshift. (*F–H*) Nuclear fluorescence driven by the *pPIF4:PIF4-GFP, pBES1:BES1-GFP, pHY5:HY5-YFP, pARF6:ARF6-GFP,* and *pARF7:ARF7-VENUS* in hypocotyl cells (*F*), *p35S:PIF4-GFP* in hypocotyl cells (*G*, including the *chl1-5* background) or *pPIF4:PIF4-GFP* in cotyledon cells (*H*), measured by confocal microscopy 6 h after the nitrate upshift (2 h included for *pPIF4:PIF4-GFP*; red shows chlorophyll fluorescence). (*I–L*) Bioluminescence driven by *pPIF4:PIF4-LUC* (*I*, *J*, and *L*, including the *chl1-5* background) or *pPIF4:LUC* (*K*) during the photoperiod of day 4 (*I* and *K*) or 1.5 h after the nitrate upshift (*J* and *L*). (*M* and *N*) PIF4-HA (*M*) and PIF4-GFP (*N*) protein blots of entire seedlings harvested 1.5 h after the application of nitrate (for quantification see *SI Appendix*, Fig. S6). (*O*) Addition of 5 μM Picloram bypasses the requirement of cotyledons for the growth promotion of Col-0 but not *pif4* hypocotyls. (*P*) Repositioning Col-0 but not *pif4* cotyledons partially restores the elongation response of Col-0 hypocotyls without cotyledons. Data are means ± SE and individual values (omitted in kinetics data). Asterisks indicate the significance of the effect of nitrate upshift in Bonferroni tests following significant interaction (int, *A–E*, *G*, *L*, *O*, and *P*), the main effect of nitrate upshift if the interaction is not significant (*F*, PIF4) or in Student's *t* tests (*F*, *I–K*, *M*, and *N*): **P* < 0.05; ***P* < 0.01; ****P* < 0.001; ns, not significant.

Using the RNA-sequencing data, we identified 397 genes with expression enhanced by the nitrate upshift in the wild type (Fig. 4*A*). The GO term "response to auxin" and the protein class "SAUR" were overrepresented among these genes. Supporting these observations the nitrate upshift enhanced auxin-induced transcriptional activity revealed by *DR5:GFP* in hypocotyl cells (Fig. 4*B*), reduced the levels of DII-VENUS (which decrease with auxin) both in hypocotyl and cotyledon cells (Fig. 4 *C* and *D*) and increased the staining driven by *pSAUR21:GUS* in hypocotyl cells (Fig. 4*E*). The GO terms overrepresented among the genes with expression reduced by the nitrate upshift included "response to water deprivation" but no functions with obvious direct relation with the growth response (Fig. 4*A*).

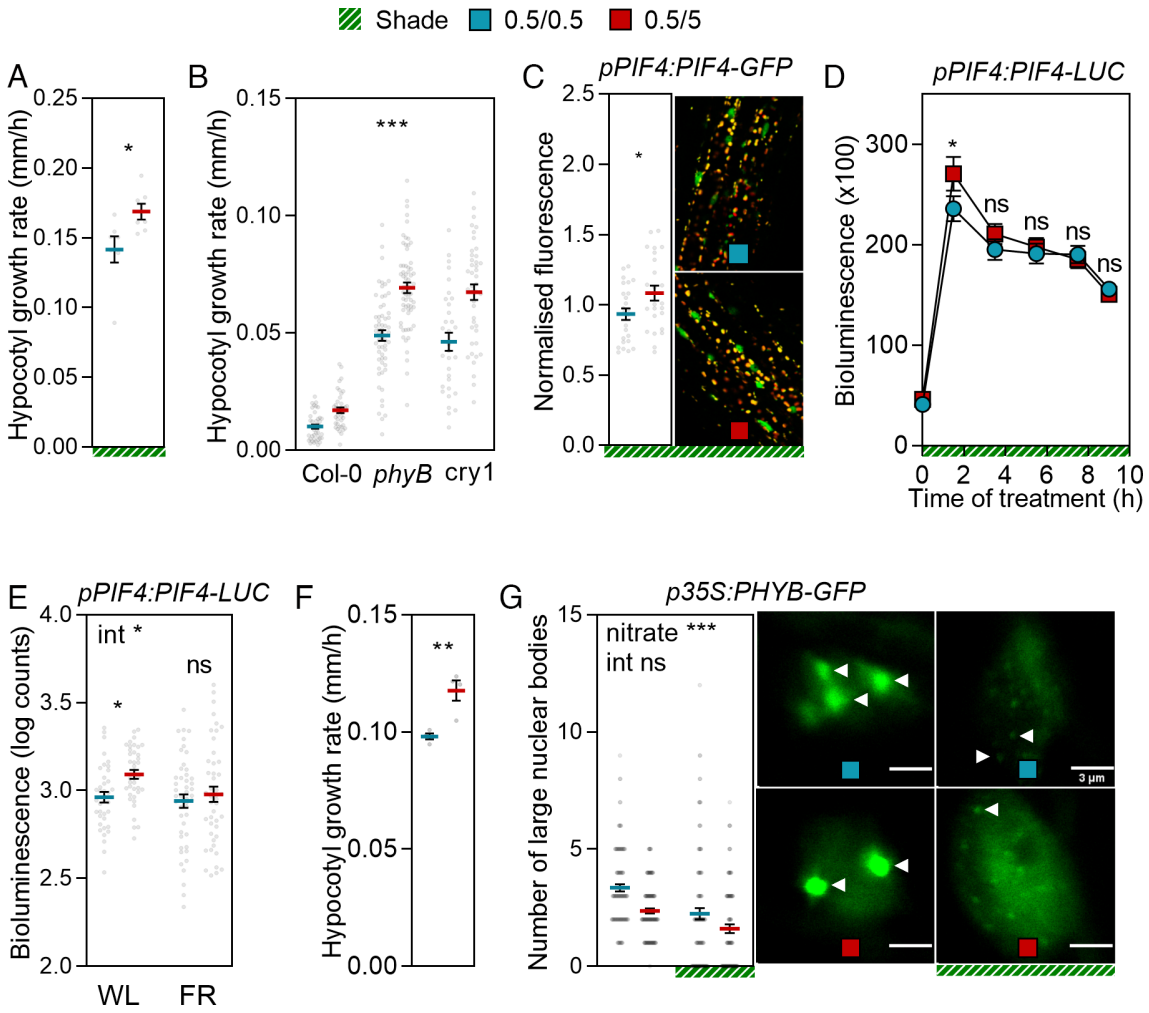

Fig. 3. The PIF4 response to nitrate requires active phyB while the growth response does not. Seedlings transferred from 0.5 mM to 5.0 mM nitrate 1 h after the beginning of the photoperiod of day 4 are compared to the controls that remained on 0.5 mM nitrate. (*A*) Hypocotyl growth rate in seedlings grown under simulated shade (transferred to shade the day before nitrate treatments). (*B*) Hypocotyl growth rate in seedlings of the wild type, *phyB,* and *cry1* mutants. (*C*) Nuclear fluorescence driven by the *pPIF4:PIF4-GFP* transgene, measured by confocal microscopy 6 h after the nitrate upshift in seedlings simultaneously transferred to simulated shade. (*D*) Kinetics of the bioluminescence driven by *pPIF4:PIF4-LUC* during the photoperiod of day 4 in seedlings that were simultaneously transferred to simulated shade. (*E*) Bioluminescence driven by *pPIF4:PIF4-LUC* 1.5 h after the beginning of the white light photoperiod (WL) and in seedlings measured simultaneously after receiving a pulse of far-red light (FR) at the subjective time of initiation of the photoperiod and followed by darkness. (*F*) Rate of hypocotyl growth in seedlings treated exactly as in *E*. (*G*) Number of small and large phyB nuclear bodies in hypocotyl cells. Data are means ± SE and individual values (*A–C*, *E*, and *F*) or means ± SE of at least 70 seedlings (four plates with control and nitrate seedlings on the same plate, *D*). Asterisks indicate the significance of the effect of nitrate in Student's *t* tests (*A*, *C*, and *D*), the main effect of nitrate in two-way ANOVA that showed no significant interaction (*B* and *G*, in *E* data were log transformed for the analysis to obtain homogeneity of variance) or the effect of nitrate in Bonferroni tests following significant interaction (int, *E*): **P* < 0.05; ***P* < 0.01; ****P* < 0.001; ns, not significant.

Many of the identified *SAUR* genes are binding targets of PIF4 (*SI Appendix*, Fig. S5*A*). The *pif4* mutation reduced the response to the nitrate upshift of seven of them, and their expression significantly correlated with the hypocotyl elongation response (Fig. 4*F*). Several *SAUR* genes that respond to nitrate are binding targets and/or require NLP7 to respond to cold (*SI Appendix*, Fig. S5 *A* and *B*). The *nlp7* mutation reduced the expression response to the nitrate upshift of *SAUR67* (also affected by PIF4) and *SAUR6* (not affected by PIF4) but not that of *SAUR21* (affected by PIF4) (Fig. 4 *G–I*).

The Hypocotyl Growth Response Requires Auxin SAUR and PP2C.D genes. Supporting a role of the observed increase in auxin signaling (Fig. 4), hypocotyl growth failed to respond to the nitrate upshift in the *shade avoidance 3* (*sav3)* and quintuple *yucca* (*yucq*) mutants, deficient in auxin synthesis (64, 65) (Fig. 5*A*). Since nitrate also increased the expression of *SAUR* genes (Fig. 4), we generated multiple *saur* CRISPR-Cas9 mutants to investigate whether the response to nitrate requires these genes. Effectively, the *saur19/21/23/24*, *saur19/20/21/22/23/24*, *saur61/62/63/64/65/66/67/68/75*, *saur19/20/21/22/23/24/61/62/63/64/65/66/67/68/75*, *saur19/20/21/22/23/24/26/27/29/61/62/63/64/65/66/67/68/73/75*, *and saur9/16/19/20/21/22/23/24/26/27/29/61/62/63/64/65/66/67/68/73/75* mutants, all failed to respond to nitrate (Fig. 5*B*). For the SAUR19 clade (SAURs 19-24), we verified this result in three independent mutant lines. Likewise, transgenic lines overexpressing SAUR19 or SAUR63 showed enhanced hypocotyl growth rate and failed to respond to nitrate (Fig. 5*B*), demonstrating the importance of proper regulation of SAUR function for the normal response to nitrate.

SAUR proteins interact physically with and inhibit the activity of the PP2C.D subfamily of type 2C protein phosphatases (PP2C.D), which in turn inhibit the activity of plasma-membrane proton ATPases that acidify the apoplast to favor cell-wall loosening (66, 67). The *pp2.cd2 pp2c.d5 pp2c.d6* mutant lacking key members of these SAUR downstream effectors showed high rates of hypocotyl growth and failed to respond to the nitrate upshift

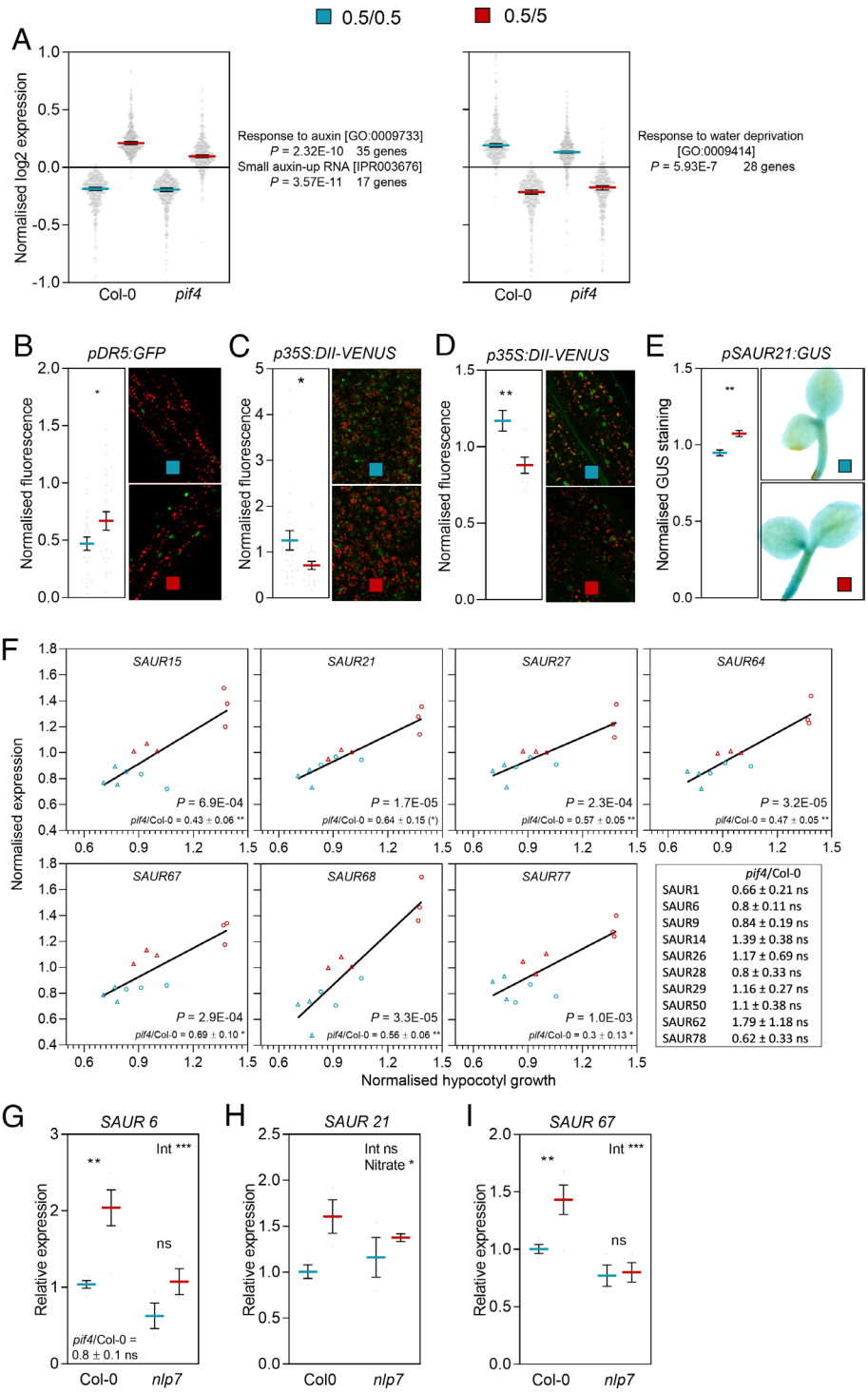

Fig. 4. The nitrate upshift enhances the expression of selected *SAUR* genes. Seedlings transferred from 0.5 mM to 5.0 mM nitrate 1 h after the beginning of the photoperiod of day 4 are compared to the controls that remained on 0.5 mM nitrate. (*A*) Genes with expression enhanced (*Left*) or reduced (*Right*) by the nitrate upshift in the wild type and the associated overrepresented gene ontology (GO) terms. Each datum point is the average expression of one gene in Col-0 or *pif4* under control or nitrate upshift conditions (three biological replicates, RNA sequencing, Dataset S1). (*B*) Nuclear fluorescence driven by the *pDR5:GFP* transgene measured by confocal microscopy 3 h after the nitrate upshift. (*C* and *D*) DII-VENUS measured by confocal microscopy in cotyledon (*C*) or hypocotyl (*D*) cells 1.5 h after the nitrate upshift. (*E*) GUS staining in the hypocotyl driven by the *pSAUR21:GUS* transgene, 3.5 h after the shift in nitrate. (*F*) Correlation between normalized *SAUR* gene expression and normalized hypocotyl growth across genotypes and nitrate conditions. Each datum point corresponds to the expression in one transcriptome experiment and the growth of the hypocotyl under the same condition during the same experiment (circles: Col-0; triangles: *pif4*). The significance of the correlation is indicated. The ratio between the response to the nitrate upshift in *pif4* and Col-0 was calculated for each experiment and the mean ± SE is indicated. (*G–I*) The *nlp7* mutation reduced the effect of the nitrate on *SAUR6* (*G*) and *SAUR67* (*H*) but not *SAUR21* (*I*) expression (measured 3.5 h after the nitrate upshift). Data are means ± SE and individual values (*A–E* and *G–I*). Asterisks indicate the significance of the effect of the nitrate upshift in Student's *t* tests (*B–E*), Bonferroni tests following significant interaction (int, *G* and *I*) or the main effect of nitrate following nonsignificant interaction (*H*): $*P < 0.05$; $**P < 0.01$; $***P < 0.001$; ns, not significant.

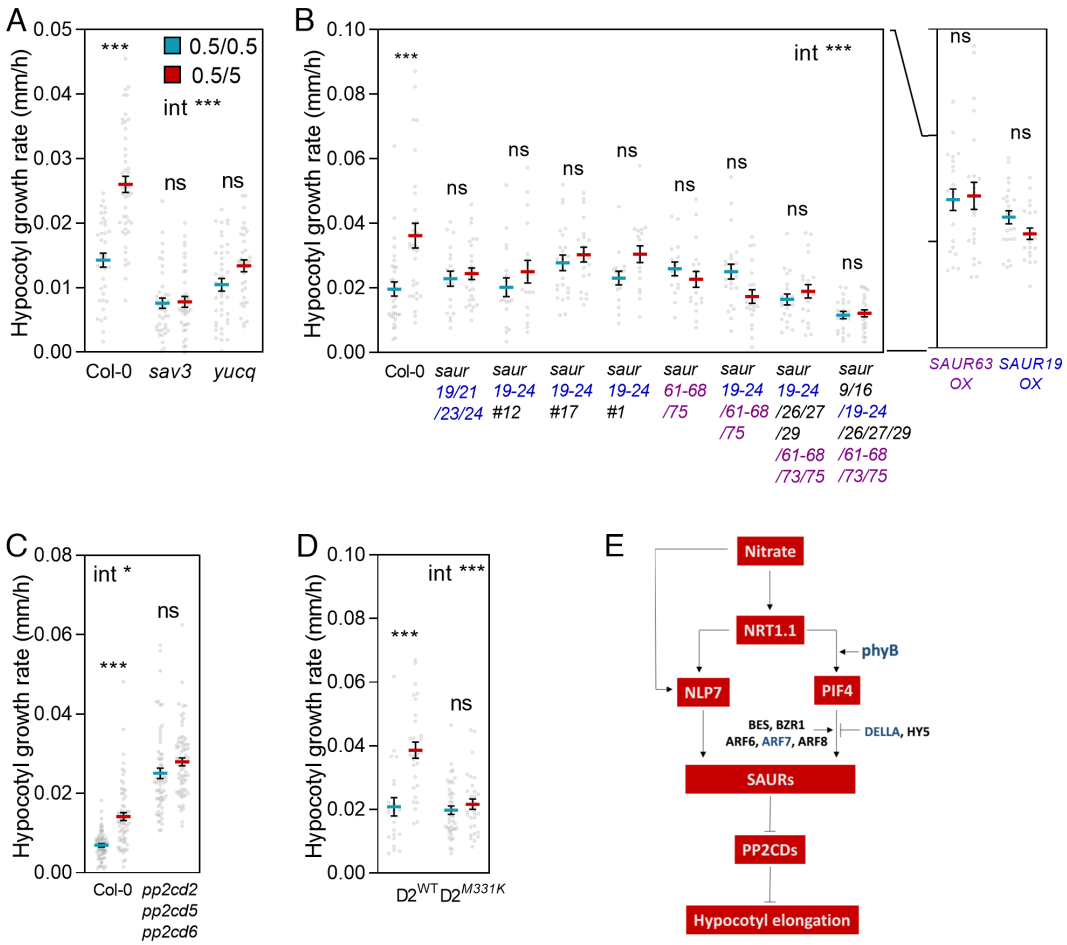

Fig. 5. The hypocotyl growth response to nitrate requires auxin, SAURS, and SAUR-regulated PP2C.Ds. Seedlings transferred from 0.5 mM to 5.0 mM nitrate 1 h after the beginning of the photoperiod of day 4 are compared to the controls that remained on 0.5 mM nitrate. Hypocotyl growth rate in seedlings of the wild type, auxin-synthesis mutants (*A*), multiple *saur* mutants or transgenic *SAUR* overexpressors (*B*, OX), multiple *pp2c.d* mutants (*C*) or multiple *pp2c.d* mutants complemented by wild-type PP2C.D2-GFP or PP2C.D2^{M331K}-GFP (*D*). (*E*) Model that integrates the results. Data are means ± SE and individual values. Asterisks indicate the significance of the effect of nitrate in Bonferroni tests following significant interaction (int): *$P < 0.05$; ***$P < 0.001$; ns, not significant.

(Fig. 5*C*). Finally, *pp2c.d2* seedlings expressing a mutant PP2C.D2-GFP derivative that abolishes SAUR binding (PP2C.D^{M331K}) showed reduced hypocotyl growth rate and failed to respond to the nitrate upshift (Fig. 5*D*).

Discussion

Although nitrate promotes the growth of the stem in many crop species (2, 35, 36), the mechanisms by which nitrate controls this agriculturally important trait were poorly understood. Using the hypocotyl of *A. thaliana* seedlings as a model, here, we show that the rate of elongation responded to upshifts in nitrate concentration via the canonical NRT1.1-NLP7 pathway (Fig. 1) and the enhancement of PIF4 abundance by posttranscriptional mechanisms (Fig. 2), to promote the expression of numerous *SAUR* genes (Fig. 4) and cell expansion (Fig. 5). This mechanism is different from those reported for root (24, 28–31) or leaf (32–32) responses to nitrate (see Introduction). The hypocotyl response increased plant stature and hence the ability to compete for light when additional nitrate becomes available.

The promotion of hypocotyl growth was specific for nitrate and required a nitrate upshift and the phosphorylated form of NRT1.1, but not its transport function (Fig. 1). NRT1.1 phosphorylation did not trigger a constitutive growth response, indicating that this condition is necessary but not sufficient and high nitrate levels are still required. Thus, at 0.5 mM, NRT1.1 would be phosphorylated (68), but hypocotyl elongation is reduced due to the absence of the high nitrate cue. Under constant 5.0 mM hypocotyl elongation is reduced presumably because at that concentration, the high nitrate cue is present but NRT1.1 is unphosphorylated (68). The shift to high nitrate promotes growth because it is predicted to combine transiently high NRT1.1 phosphorylation (68) and high nitrate. In support of this hypothesis, a phosphomimetic allele of NRT1.1 showed enhanced hypocotyl elongation in response to continuous high nitrate, a condition that was not effective in the wild type.

PIF4 levels increased in the hypocotyl cells (Fig. 2), where it was required for the nitrate response likely because its ability to directly bind *SAUR* gene promoters and enhance their activity (49). In addition, the nitrate upshift increased PIF4 levels in the cotyledons (Fig. 2), where it was also required for the hypocotyl growth response, likely due to its positive effect on auxin synthesis (37, 39). The observed effects of the nitrate upshift on DII-VENUS and *pDR5:GFP* activity (Fig. 4) and the bypass of the cotyledon requirement by Picloram (Fig. 2) are consistent with this possibility.

The regulation of nitrate metabolism by phytochrome signaling is well established (69). Conversely, here, we show that nitrate regulates phyB and PIF4. The PIF4 response to the nitrate upshift required active phyB (Fig. 3). The active form of the light and temperature sensor phyB undergoes liquid–liquid phase separation to form nuclear droplets, where it selectively recruits interacting

partners like PIF4 (62). Large phyB nuclear bodies form when phyB activity is high (63). phyB negatively regulates PIF4 stability by favoring its phosphorylation and degradation in the 26S proteasome (70). Since the nitrate upshift reduced the abundance of large phyB nuclear bodies, we hypothesize that it could reduce phyB-mediated induction of PIF4 degradation; however, the post-transcriptional mechanisms by which NRT1.1 affects PIF4 remain to be elucidated.

The growth response also required BES1, BZR1, ARF6, ARF7, ARF8, DELLA, and HY5 (Fig. 2). At least BZR1 and ARF6 physically interact with PIF4 synergistically controlling gene expression (e.g., the promotion of *SAUR15* expression) and are negatively regulated by DELLA proteins (47–50). HY5 and PIF4 antagonistically regulate common gene targets through direct binding to the same cis element (51). Thus, the growth response to the nitrate upshift would require positive and negative regulators of PIF4 to maximize its impact on hypocotyl elongation. ARFs would also mediate the elevated transcriptional response to auxin (71) (Fig. 4). The nuclear abundance of two of these regulators (ARF7 and RGA) responded to the nitrate upshift.

During the green revolution, breeders introduced dwarfing gain-of-function mutant alleles of DELLA genes into elite wheat cultivars to reduce lodging (8). Here, we show that the DELLA protein RGA increases its abundance in the hypocotyl in response to nitrate upshifts. DELLAs negatively regulate PIF4 (47), required for the growth response (Fig. 2*A*). This means that the approach used during the green revolution was basically an upgrade of a mechanism that already existed in nature. The use of DELLA has drawbacks because it reduces nitrogen use efficiency (9–12). Since SAURs work downstream of the PIF-DELLA module, they could offer targets to seek for cultivars resistant to nitrogen-induced lodging but without reduced nitrogen-use efficiency.

Materials and Methods

Plant Material. We used with *A. thaliana* Col-0 as wild type and mutants and transgenic lines in the same background, unless indicated otherwise (*SI Appendix*, Table S1).

Growth Conditions. Seeds were sown on filter paper or nylon mesh in contact with 25 mL of 0.8% agar in transparent plastic boxes (85 mm × 45 mm) or 200 µL of 0.8% agar per well of 96-well microplates (Greiner Lumitrac 600, luminometer experiments). The agar contained 0.5 or 5.0 mM KNO_3 (as indicated). Then, the seeds were stratified at 5 °C in darkness for 2 to 5 d and placed in a growth chamber at 22 °C and a white light photoperiod of 10 h provided by an array of LED and halogen lamps. The photosynthetically active radiation (400 to 700 nm) was 120 µmol m^{-2} s^{-1}, and the red/far-red ratio was 1.1.

Nitrogen Treatments. One hour after the beginning of day 4, all the seedlings (including the controls that did not change the features of their substrate) were transferred on filter paper or nylon mesh from the initial medium to a new medium (0.8% agar, pH 6.2) with the final concentration of KNO_3, KCl, NH_4Cl, or glutamine indicated in each case.

Hypocotyl Growth Rate. To determine the growth rate of the hypocotyl, after stratification, the boxes were turned to place with the agar vertically. The seedlings were photographed from their side on a fixed support with a digital camera (Nikon D5600 with the AF-S Micro-Nikkor 60 mm f/2.8 G ED lens) at the beginning of treatment and at the end of the photoperiod of that day (unless otherwise indicated). The length of each hypocotyl was measured with Fiji (72) at each time point, and the difference was calculated and divided by the number of hours between successive measurements to calculate the growth rate. In cotyledon growth experiments, the agar remained at the horizontal position throughout the experiments, and the seedlings were photographed from above. In experiments involving different nitrate (or nitrogen) treatments applied only to the wild type, each biological replicate is the pooled data of all the seedlings of the growth box. In experiments comparing the response to nitrate of different genotypes, each seedling is a replicate because all the genotypes were in the same growth box.

Gene Expression by Real-Time PCR. At least three biological samples of approximately 100 seedlings were harvested from each treatment between 2 and 6 h from the beginning of the nitrate treatment and frozen in liquid nitrogen; the total RNA was extracted with the Spectrum Plant Total RNA Kit (Sigma-Aldrich) and subjected to a DNase treatment with RQ1 RNase-Free DNase (Promega). From this RNA, cDNA was synthesized using M-MLV (Promega) and oligo-dT. The synthesized cDNAs were amplified with FastStart Universal SYBRGreenMaster (Roche) using an ABI PRISM 7500 Real-Time PCR System (Applied Biosystems). UBQ10 was used as housekeeping, and the expression was calculated as $2^{-\Delta\Delta CT}$ (73).

RNA Sequencing. Seedlings of three biological replicates (different dates) of Col-0 and *pif4-101* were harvested and fixed 3.5 h after the beginning of the nitrate upshift in 90% cold acetone under vacuum. Fixed seedlings were dissected in ethanol 70% to separate hypocotyls, which were recovered in ethanol 100%. The RNA was extracted with the Spectrum Plant Total RNA Kit (Sigma-Aldrich). The construction of libraries and sequencing (100 bp, paired end) were performed by Beijing Genomics Institute China using the BGIseq500 platform, obtaining approximately 50,000,000 reads in each sample. The reads were aligned to the Arabidopsis genome (TAIR10) using HISAT2 (74) and counts were calculated with Htseq (75). Pearson's correlation coefficients between replicate samples were >0.99 and were significant at $P < 0.0001$.

Confocal Microscopy. We followed the protocols previously established (63, 76). Briefly, an LSM 510 Meta (Zeiss) or LSM 710 (Zeiss) laser scanning confocal microscope was used with an EC Plan-Neofluar 40×/1.3 lens. GFP and YFP marks were excited by an argon laser (λ = 488 nm) and emission detected from 505 to 530 nm. VENUS was excited by the argon laser (λ = 514 nm) and emission detected from 525 to 580. Chloroplasts were visualized by exciting the chlorophyll with a He–Ne laser (λ = 543 nm) and emission detected above 560 nm. The images were analyzed with Fiji software (72). When required to keep the timing of sampling, seedlings were fixed as described in *SI Appendix*, Materials and Methods, Fixation for Confocal Microscopy.

β-glucuronidase Activity. Transgenic seedlings bearing the β-glucuronidase (GUS) reporter were fixed, stained, and photographed as described in *SI Appendix*, Materials and Methods, β-glucuronidase Activity. Each replicate corresponds to the average of the seedlings of one growth box normalized to the average of all the boxes of each experiment.

Luciferase Activity. Luciferase activity assays were conducted using a Centro XS^3 LB 960 Berthold microplate luminometer as described in *SI Appendix*, Materials and Methods, Luciferase Activity. Each seedling was randomly assigned to the different wells of the microplate and used as replicate in statistics.

Protein Blots. Proteins were extracted, separated in SDS gels, transferred, and revealed with primary and secondary antibodies as described in *SI Appendix*, Materials and Methods, Protein Blots. Immunoblot bands were quantified by using ImageJ software and normalized band intensity against the corresponding antiactin immunoblot bands for each sample (see *SI Appendix*, Fig. S6 for details of quantification and normalization).

Statistics. The criteria used for replication and normalization are indicated above for each output variable. The specific tests applied in each instance are indicated in the legends of the figures and further described in *SI Appendix*, Materials and Methods, Statistics.

Data, Materials, and Software Availability. RNA sequencing data have been deposited in National Center for Biotechnology Information (NCBI) Sequence Read Archive (SRA) (PRJNA997577) (77). All study data are included in the article and/or supporting information.

ACKNOWLEDGMENTS. We thank Colby Starker and Daniel Voytas (University of Minnesota, US) for generating the pCGS833 CRISPR construct. We thank Jian Hua (Cornell University, US) for sending seeds of the *saur26/27/29/73* mutant, Ning Wei (Southwest University of Chongqing, China) for sending seeds of the

saur19/20/21/22/23/24 #12 and *#17* mutants and Malcom Bennet (University of Nottingham, UK) for sending seeds of the *pARF7:ARF7-VENUS* line. Part of this work is included in the Doctoral Thesis of M.E.P. (*Facultad de Ciencias Agrarias, Universidad Nacional de Mar del Plata*). Supported by University of Buenos Aires (grant 20020170100505BA to J.J.C.), *Agencia Nacional de Promoción Científica y Tecnológica* (ANPCYT, grants PICT-2018-01695 and PICT-2021-I-A-01070 to J.J.C.), NIH (grants GM145298 and GM067203 to W.M.G.), and US NSF (grant MCB-1615557 to J.W.R.).

Author affiliations: [a]Instituto de Investigaciones Fisiológicas y Ecológicas Vinculadas a la Agricultura, Facultad de Agronomía, Universidad de Buenos Aires, Consejo Nacional de Investigaciones Científicas y Técnicas, Buenos Aires 1417, Argentina; [b]Fundación Instituto Leloir, Instituto de Investigaciones Bioquímicas de Buenos Aires, Consejo Nacional de Investigaciones Científicas y Técnicas, Buenos Aires 1405, Argentina; [c]Department of Biology, University of North Carolina, Chapel Hill, NC 27599-3280; [d]Department of Plant and Microbial Biology, University of Minnesota, St. Paul, MN 55108; [e]Instituto de Biologia Molecular y Celular de Plantas, Consejo Superior de Investigaciones Científicas, Universidad Politécnica de Valencia, Valencia 46022, Spain; and [f]Departamento de Genética Molecular y Microbiología, Facultad de Ciencias Biológicas, Pontificia Universidad Católica de Chile, Santiago 8331150, Chile

1. S. Rajkumara, Lodging in cereals–A review. *Agric. Rev.* **29**, 55–60 (2008).
2. M. Zhang *et al.*, Effect of nitrogen levels and nitrogen ratios on lodging resistance and yield potential of winter wheat (Triticum aestivum L.). *PLoS One* **12**, e0187543 (2017).
3. J. Zhang *et al.*, Lodging resistance characteristics of high-yielding rice populations. *Field Crop. Res.* **161**, 64–74 (2014).
4. X.-m. Liu, W.-r. Gu, C.-f. Li, J. Li, S. Wei, Effects of nitrogen fertilizer and chemical regulation on spring maize lodging characteristics, grain filling and yield formation under high planting density in Heilongjiang Province, China. *J. Integr. Agric.* **20**, 511–526 (2021).
5. E. Schultz *et al.*, Response of sunflower to nitrogen and phosphorus in north Dakota. *Agron. J.* **110**, 685–695 (2018).
6. S. Khan *et al.*, Alteration in yield and oil quality traits of winter rapeseed by lodging at different planting density and nitrogen rates. *Sci. Rep.* **8**, 1–12 (2018).
7. G. S. Khush, Green revolution: Preparing for the 21st century. *Genome* **42**, 646–655 (1999).
8. P. Hedden, The genes of the Green Revolution. *Trends Genet.* **19**, 5–9 (2003).
9. S. Li *et al.*, Modulating plant growth–metabolism coordination for sustainable agriculture. *Nature* **560**, 595–600 (2018).
10. H. Xue, Y. Zhang, G. Xiao, Neo-gibberellin signaling: Guiding the next generation of the Green Revolution. *Trends Plant Sci.* **25**, 520–522 (2020).
11. M. J. Gooding, M. Addisu, R. K. Uppal, J. W. Snape, H. E. Jones, Effect of wheat dwarfing genes on nitrogen-use efficiency. *J. Agric. Sci.* **150**, 3–22 (2012).
12. Q. Liu *et al.*, Improving crop nitrogen use efficiency toward sustainable Green Revolution. *Annu. Rev. Plant Biol.* **73**, 523–551 (2022).
13. K. G. Cassman, A. Dobermann, D. T. Walters, Agroecosystems, nitrogen-use efficiency, and nitrogen management. *Ambio* **31**, 132–140 (2002).
14. H. J. Di, K. C. Cameron, Nitrate leaching in temperate agroecosystems: Sources, factors and mitigating strategies. *Nutr. Cycl. Agroecosystems* **64**, 237–256 (2002).
15. J. A. A. O'Brien *et al.*, Nitrate transport, sensing, and responses in plants. *Mol. Plant* **9**, 837–856 (2016).
16. S. F. Undurraga, C. Ibarra-henríquez, I. Fredes, J. M. Álvarez, R. A. Gutiérrez, Nitrate signaling and early responses in Arabidopsis roots. *J. Exp. Bot.* **68**, 1–11 (2017).
17. C. H. Ho, S. H. Lin, H. C. Hu, Y. F. Tsay, CHL1 functions as a nitrate sensor in plants. *Cell* **138**, 1184–1194 (2009).
18. E. Bouguyon *et al.*, Multiple mechanisms of nitrate sensing by Arabidopsis nitrate transceptor NRT1.1. *Nat. Plants* **1**, 2–9 (2015).
19. X. Zhang *et al.*, Phosphorylation-mediated dynamics of nitrate transceptor NRT1.1 regulate auxin flux and nitrate signaling in lateral root growth. *Plant Physiol.* **181**, 480–498 (2019).
20. J. Sun *et al.*, Crystal structure of the plant dual-affinity nitrate transporter NRT1.1. *Nature* **507**, 73–77 (2014).
21. J. L. Parker, S. Newstead, Molecular basis of nitrate uptake by the plant nitrate transporter NRT1.1. *Nature* **507**, 68–72 (2014).
22. K. H. Liu, Y. F. Tsay, Switching between the two action modes of the dual-affinity nitrate transporter CHL1 by phosphorylation. *EMBO J.* **22**, 1005–1013 (2003).
23. K. Liu *et al.*, Discovery of nitrate–CPK–NLP signalling in central nutrient–growth networks. *Nature* **545**, 311–316 (2017).
24. L. Castaings *et al.*, The nodule inception-like protein 7 modulates nitrate sensing and metabolism in Arabidopsis. *Plant J.* **57**, 426–435 (2009).
25. J. M. Alvarez *et al.*, Transient genome-wide interactions of the master transcription factor NLP7 initiate a rapid nitrogen-response cascade. *Nat. Commun.* **11**, 1–13 (2020).
26. K. Liu *et al.*, NIN-like protein 7 transcription factor is a plant nitrate sensor. *Science* **9**, 1419–1425 (2022).
27. X. Wang *et al.*, A transceptor–channel complex couples nitrate sensing to calcium signaling in Arabidopsis. *Mol. Plant* **14**, 774–786 (2021).
28. E. A. Vidal *et al.*, Nitrate-responsive miR393/AFB3 regulatory module controls root system architecture in Arabidopsis thaliana. *Proc. Natl. Acad. Sci. U.S.A.* **107**, 4477–4482 (2010).
29. G. Krouk *et al.*, Nitrate-regulated auxin transport by NRT1.1 defines a mechanism for nutrient sensing in plants. *Dev. Cell* **18**, 927–937 (2010).
30. A. Vega *et al.*, Nitrate triggered phosphoproteome changes and a PIN2 phosphosite modulating root system architecture. *EMBO Rep.* **22**, 1–19 (2021).
31. E. A. Vidal *et al.*, Nitrate in 2020: Thirty years from transport to signaling networks. *Plant Cell* **32**, 2094–2119 (2020).
32. S. Moreno *et al.*, Nitrate defines shoot size through compensatory roles for endoreplication and cell division in Arabidopsis thaliana. *Curr. Biol.* **30**, 1988–2000.e3 (2020).
33. R. Abualia *et al.*, Molecular framework integrating nitrate sensing in root and auxin-guided shoot adaptive responses. *Proc. Natl. Acad. Sci. U.S.A.* **119**, 1–11 (2022).
34. Y. Liu *et al.*, Diverse nitrogen signals activate convergent ROP2-TOR signaling in Arabidopsis. *Dev. Cell* **56**, 1283–1295.e5 (2021).
35. D. Euring, H. Bai, D. Janz, A. Polle, Nitrogen-driven stem elongation in poplar is linked with wood modification and gene clusters for stress, photosynthesis and cell wall formation. *BMC Plant Biol.* **14**, 1–13 (2014).
36. W. Zhang *et al.*, Lodging resistance of Japonica rice (Oryza sativa L.): Morphological and anatomical traits due to top-dressing nitrogen application rates. *Rice* **9**, 1–11 (2016).
37. K. A. Franklin *et al.*, PHYTOCHROME-INTERACTING FACTOR 4 (PIF4) regulates auxin biosynthesis at high temperature. *Proc. Natl. Acad. Sci. U.S.A.* **108**, 20231–20235 (2011).
38. S. Lorrain, T. Allen, P. D. Duek, G. C. Whitelam, C. Fankhauser, Phytochrome-mediated inhibition of shade avoidance involves degradation of growth-promoting bHLH transcription factors. *Plant J.* **53**, 312–323 (2008).
39. P. Hornitschek *et al.*, Phytochrome interacting factors 4 and 5 control seedling growth in changing light conditions by directly controlling auxin signaling. *Plant J.* **71**, 699–711 (2012).
40. A. S. Fiorucci *et al.*, PHYTOCHROME INTERACTING FACTOR 7 is important for early responses to elevated temperature in Arabidopsis seedlings. *New Phytol.* **226**, 50–58 (2020).
41. L. Li *et al.*, Linking photoreceptor excitation to changes in plant architecture. *Genes Dev.* **26**, 785–790 (2012).
42. X. Huang *et al.*, Shade-induced nuclear localization of PIF7 is regulated by phosphorylation and 14-3-3 proteins in Arabidopsis. *Elife* **7**, e31636 (2018).
43. B. Y. W. Chung *et al.*, An RNA thermoswitch regulates daytime growth in Arabidopsis. *Nat. plants* **6**, 522 (2020).
44. J. W. Reed *et al.*, Three auxin response factors promote hypocotyl elongation. *Plant Physiol.* **178**, 864–875 (2018).
45. C. Costigliolo Rojas *et al.*, Organ-specific COP1 control of BES1 stability adjusts plant growth patterns under shade or warmth. *Dev. Cell* **57**, 2009–2025.e6 (2022).
46. C. Ibañez *et al.*, Brassinosteroids dominate hormonal regulation of plant thermomorphogenesis via BZR1. *Curr. Biol.* **28**, 303–310.e3 (2018).
47. M. De Lucas *et al.*, A molecular framework for light and gibberellin control of cell elongation. *Nature* **451**, 480–484 (2008).
48. J. Gallego-Bartolomé *et al.*, Molecular mechanism for the interaction between gibberellin and brassinosteroid signaling pathways in Arabidopsis. *Proc. Natl. Acad. Sci. U.S.A.* **109**, 13446–13451 (2012).
49. E. Oh, J. Y. Zhu, Z. Y. Wang, Interaction between BZR1 and PIF4 integrates brassinosteroid and environmental responses. *Nat. Cell Biol.* **14**, 802–809 (2012).
50. E. Oh *et al.*, Cell elongation is regulated through a central circuit of interacting transcription factors in the Arabidopsis hypocotyl. *Elife* **3**, e03031 (2014).
51. G. Toledo-Ortiz *et al.*, The HY5-PIF regulatory module coordinates light and temperature control of photosynthetic gene transcription. *PLoS Genet.* **10**, e1004416 (2014).
52. E. Bouguyon *et al.*, Multiple mechanisms of nitrate sensing by Arabidopsis nitrate transceptor NRT1.1. *Nat. Plants* **1**, 15015 (2015).
53. M. Okamoto, J. J. Vidmar, A. D. M. Glass, Regulation of NRT1 and NRT2 gene families of Arabidopsis thaliana: Responses to nitrate provision. *Plant Cell Physiol.* **44**, 304–317 (2003).
54. R. Wang, M. Okamoto, X. Xing, N. M. Crawford, Microarray analysis of the nitrate response in Arabidopsis roots and shoots reveals over 1,000 rapidly responding genes and new linkages to glucose, trehalose-6-phosphate, iron, and sulfate metabolism. *Plant Physiol.* **132**, 556–567 (2003).
55. Y. F. Tsay, J. I. Schroeder, K. A. Feldmann, N. M. Crawford, The herbicide sensitivity gene CHL1 of arabidopsis encodes a nitrate-inducible nitrate transporter. *Cell* **72**, 705–713 (1993).
56. E. Bouguyon *et al.*, Nitrate controls root development through posttranscriptional regulation of the NRT1.1/NPF6.3 transporter/sensor. *Plant Physiol.* **172**, 1237–1248 (2016).
57. D. E. Gras *et al.*, SMZ/SNZ and gibberellin signaling are required for nitrate-elicited delay of flowering time in Arabidopsis thaliana. *J. Exp. Bot.* **69**, 619–631 (2018).
58. J. J. Casal, Photoreceptor signaling networks in plant responses to shade. *Annu. Rev. Plant Biol.* **64**, 403–427 (2013).
59. E. S. Burgie, R. D. Vierstra, Phytochromes: An atomic perspective on photoactivation and signaling. *Plant Cell* **26**, 568–4583 (2014).
60. H. Liu, B. Liu, C. Zhao, M. Pepper, C. Lin, The action mechanisms of plant cryptochromes. *Trends Plant Sci.* **16**, 684–691 (2011).
61. J. J. Casal, M. A. Mazzella, Conditional synergism between cryptochrome 1 and phytochrome B is shown by the analysis of phyA, phyB, and hy4 simple, double, and triple mutants in Arabidopsis. *Plant Physiol.* **118**, 19–25 (1998).
62. D. Chen *et al.*, Integration of light and temperature sensing by liquid-liquid phase separation of phytochrome B. *Mol. Cell* **82**, 3015–3029.e6 (2022).
63. M. Legris *et al.*, Phytochrome B integrates light and temperature signals in Arabidopsis. *Science* **354**, 897–900 (2016).
64. Y. Cheng, X. Dai, Y. Zhao, Auxin synthesized by the YUCCA flavin monooxygenases is essential for embryogenesis and leaf formation in Arabidopsis. *Plant Cell* **19**, 2430–2439 (2007).
65. Y. Tao *et al.*, Rapid synthesis of auxin via a new tryptophan-dependent pathway is required for shade avoidance in plants. *Cell* **133**, 164 (2008).
66. A. K. Spartz *et al.*, SAUR inhibition of PP2C-D phosphatases activates plasma membrane H+-ATPases to promote cell expansion in Arabidopsis. *Plant Cell* **26**, 2129–2142 (2014).
67. J. H. Wong, A. K. Spartz, M. Y. Park, M. Du, W. M. Gray, Mutation of a conserved motif of PP2C.D phosphatases confers SAUR immunity and constitutive activity. *Plant Physiol.* **181**, 353–366 (2019).
68. M. Rashid *et al.*, Feedforward control of plant nitrate transporter NRT1.1 biphasic adaptive activity. *Biophys. J.* **118**, 898–908 (2020).
69. C. Lillo, Signalling cascades integrating light-enhanced nitrate metabolism. *Biochem. J.* **415**, 11–19 (2008).
70. V. N. Pham, P. K. Kathare, E. Huq, Phytochromes and phytochrome interacting factors. *Plant Physiol.* **176**, 1025–1038 (2018).

71. D. Weijers, D. Wagner, Transcriptional responses to the auxin hormone. *Annu. Rev. Plant Biol.* **67**, 539–574 (2016).
72. J. Schindelin *et al.*, Fiji: An open-source platform for biological-image analysis. *Nat. Methods* **9**, 676–682 (2012).
73. K. J. Livak, T. D. Schmittgen, Analysis of relative gene expression data using real-time quantitative PCR and the 2-ΔΔCT method. *Methods* **25**, 402–408 (2001).
74. D. Kim, J. M. Paggi, C. Park, C. Bennett, S. L. Salzberg, Graph-based genome alignment and genotyping with HISAT2 and HISAT-genotype. *Nat. Biotechnol.* **37**, 907–915 (2019).
75. G. H. Putri, S. Anders, P. T. Pyl, J. E. Pimanda, F. Zanini, Analysing high-throughput sequencing data in Python with HTSeq 2.0. *Bioinformatics* **38**, 2943–2945 (2022).
76. M. Pacín, M. Semmoloni, M. Legris, S. A. Finlayson, J. J. Casal, Convergence of CONSTITUTIVE PHOTOMORPHOGENESIS 1 and PHYTOCHROME INTERACTING FACTOR signalling during shade avoidance. *New Phytol.* **211**, 967–979 (2016).
77. M. E. Pereyra, J. J. Casal, Effect of nitrate upshift and pif4 mutation on hypocotyl transcriptome. *NCBI*. https://www.ncbi.nlm.nih.gov/bioproject/PRJNA997577. Deposited 22 July 2023.